IEEE Access
Multidisciplinary | Rapid Review | Open Access Journal

Received December 18, 2019, accepted January 10, 2020, date of publication January 14, 2020, date of current version February 14, 2020.

Digital Object Identifier 10.1109/ACCESS.2020.2966529

An Optimization Tendency Guiding Mode Decomposition Method for Bearing Fault Detection Under Varying Speed Conditions

XINGXING JIANG, WENJUN GUO, GUIFU DU, JUANJUAN SHI, AND ZHONGKUI ZHU
School of Rail Transportation, Soochow University, Suzhou 215131, China

Corresponding author: Guifu Du (gfdu@suda.edu.cn)

This work was supported in part by the National Natural Science Foundation of China under Grant 51705349, Grant 51875376, and Grant 51605319, in part by the China Postdoctoral Science Foundation under Grant 2019T120456, in part by the Suzhou Prospective Research Program under Grant SYG201932, and in part by the Postgraduate Research and Practice Innovation Program of Jiangsu Province under Grant KYCX18_2502.

ABSTRACT Tacholess order tracking techniques based on time-frequency (TF) ridge detection have been extensively used in bearing fault diagnosis under varying speed conditions for decades. However, the signal components of a fault bearing related to shaft rotational frequency (SRF) is difficult to be accurately extracted by these methods because of TF resolution limitation and strong noise interference. A new TF decomposing algorithm, that is, variational nonlinear chirp mode decomposition (VNCMD) is effective to extract the time-varying feature under limited TF resolution. However, its performance is influenced by prior knowledge of initial parameters. Besides, ridge information hidden in noise is difficult to be mined effectively, which increases the difficulty of ridge extraction. In this study, a feature isolation technology is proposed to enhance fault-related features and reduce the interference of noise and irrelevant components. Then inspired by the decomposing properties research on the convergence characteristics of VNCMD, an optimization tendency guiding mode decomposition (OTGMD) method is proposed to track the instantaneous frequency (IF) of fault-related mode, which can alleviate the personnel experience requirement and is not affected by the set of TF resolution. The proposed method mainly consists of three steps. First, SRF-related information is highlighted through low-pass filtering, and the dominant IF is achieved through ridge detection method. Subsequently, for the convenience of mode extraction, the fault characteristic is augmented through iterative envelope analysis. Then, the OTGMD optimization strategy is developed to gradually decompose the target mode on the basis of the above process. Finally, a stopping criterion based on characteristic frequency ratios (CFRs) is constructed to adaptively terminate the iteration process. Simulation and experiments demonstrate that the proposed method is effective and suitable for bearing fault diagnosis under varying speed conditions.

INDEX TERMS Bearing fault diagnosis, adaptive decomposition strategy, instantaneous frequency estimation, varying speed condition.

I. INTRODUCTION

Rolling bearings are extensively used components in rotating machines, including wind turbines and electric motors [1]–[4]. They are prone to failures under harsh working environments, such as high rotating speed, heavy load and contamination, thereby leading to machine breakdowns or even fatal accidents [5], [6]. Therefore, fault detection of rolling bearings has been widely conducted to prevent accidents and reduce economic losses [7].

When a local defect is generated in bearings, the impacts between the defect and the mating surface will stimulate an impulsive signature in the vibration signal. Usually, the impulses appear periodically or quasi-periodically at a certain frequency called fault characteristic frequency (FCF) under constant speed conditions. For a fault bearing, FCF is related to shaft rotational frequency (SRF) and bearing parameters, that is, the characteristic frequency ratio (CFR)

The associate editor coordinating the review of this manuscript and approving it for publication was Abdel-Hamid Soliman.

of FCF to SRF is constant and only determined by geometric parameters. Many vibration-based techniques, such as time-domain methods [8], [9], frequency-domain methods [10], [11], deep neural networks [12], and time-frequency mode decomposition [13], [14], have been constructed to detect bearing faults for the accurate extraction of FCF. However, most of these methods only show their effectiveness for fault diagnosis under constant speed conditions. When bearings operate at varying speeds, FCF also varies with time and the signal shows non-stationary characteristics. This change will lead to an unsatisfactory result that FCF will be hardly observable and detected from the frequency spectrum, thereby resulting in spectral smearing. Thus, advanced fault diagnosis methods for varying speed conditions have been widely investigated in the past few years.

Order analysis has become the focus in fault diagnosis of rolling bearings subjected to varying speed conditions [15]. Its core idea is to perform resampling of raw vibration signals with a constant angle increment to eliminate the nonstationary effects of speed fluctuation. On this basis, spectral smearing can be solved, and conventional Fourier transform-based techniques still be applicable. Although order analysis is theoretically concise and practicable, it cannot be performed without the phase reference, which is usually acquired using tachometers. The application of auxiliary devices inevitably increases the facility costs and installation complexity. To address such problems, some tacholess approaches based on time–frequency (TF) representation (TFR) of vibration signals have been developed to extract the SRF-related features recently [16]–[19]. For instance, Zhao *et al.* [20] combined adaptive short-time Fourier transform (STFT) and generalized demodulation (GD) method for variable-speed bearing fault diagnosis. Huang *et al.*[21] employed a fast path optimization approach to estimate multiple instantaneous frequency (IF) ridges for bearing fault diagnosis under varying rotational speeds. Jiang and Li [22] and Jiang *et al.* [23] exploited a ridge fusion strategy and a dual path optimization ridge estimation method to estimate robust IF ridges for detecting the fault of planetary gearbox. Most of the above methods indicate that the corresponding IF extraction is a crucial problem in fault type identification under varying speed conditions. The results of TF ridge extraction, which are influenced by TFR resolution, may be unsatisfactory for the identification of fault types because Heisenberg's uncertainty principle inevitably exists in conventional TF analysis methods. Therefore, a method that is independent from TFR should be developed to accurately estimate IFs.

To address these issues, the adaptive signal process methods have attracted wide attentions recently [24]–[26], among which a reliable and efficient approach called variational nonlinear chirp mode decomposition (VNCMD) is explored for adaptive decomposition of multicomponent signals. It was proved that the VNCMD can be ameliorated to iteratively optimize the coarse pre-IF for bearing fault diagnosis under varying speed conditions [27]. However, the choice of initial parameters (e.g. initial IFs and decomposition number) considerably influences the decomposition results of VNCMD. Thus, an adaptive chirp mode pursuit algorithm is proposed to initialize the IF based on Hilbert transform and design an adaptive bandwidth parameter [28]. However, this method is limited because of poor initial IF caused by strong noise, which can be further improved by using ridge extraction approaches. Besides, the stopping criterion according to residual energy may result in decomposing unexpected modes. Aiming at solving the drawbacks of the aforementioned methods, a new decomposition strategy called optimization tendency guiding mode decomposition (OTGMD) method is proposed in this study to adaptively and accurately extract IFs of all meaningful modes. It minimizes the influence of initial parameters of VNCMD and interference from human experience. Concretely, the SRF-related information is first highlighted through low-pass filtering and then an iterative envelope analysis procedure is applied to enhance the fault features for more reliable identification of IF ridges information from the TFR. It can efficiently eliminate the interference of irrelevant components and demodulate the impulse response to the low-frequency band [5], [29]. Therefore, the accuracy of ridge detection methods used to extract the IF curves from the enhanced TFR is increased. Subsequently, the OTGMD method adopts a recursive decomposition scheme to extract the fault-related features. Finally, considering the interference of SRF and FCF harmonics, a novel stopping criterion is constructed to adaptively terminate decomposition on the basis of CFRs repository. Consequently, the proposed method presents the following advantages. (1) The algorithm do not require the input of the number of modes and adaptively selects the optimal initial IFs. (2) The OTGMD method is independent of TFR and resampling, thereby the accuracy of IF estimation is not influenced by the limitation of TF resolution and interpolation error. (3) The proposed method avoids specifying initial IFs for the remaining target ridges, that is, it adaptively selects the initial IFs of meaningful modes in the entire frequency band.

The rest of this paper is arranged as follows. Section II presents the brief descriptions of VNCMD method and its characteristic analysis. Then, the proposed OTGMD for bearing fault diagnosis procedure is introduced in Section III. Simulations and experimental cases are discussed in Sections IV and V for the validation. Finally, Section VI provides the conclusions.

II. THEORETICAL FRAMEWORK

A. BRIEF INTRODUCTION OF VNCMD

VNCMD is designed for wide-band signal analysis, thereby avoiding the limitation of narrow-band property in variational mode decomposition (VMD). Coincidentally, the meaningful mode buried in the vibration data measured from rolling bearings under varying speed conditions is presented as a wide-band feature in which its IF varies over a wide range of time. Therefore, the VNCMD method has been

introduced for bearing fault diagnosis under varying speed conditions.

In general, For a wide-band signal

$$x(t) = \sum_{m=1}^{K} A_m(t) \cos\left(2\pi \int_0^t f_m(\tau) d\tau + \theta_m\right) + n(t),$$

it consists of several modes and can be transformed into a narrow-band signal by demodulation techniques as follow:

$$x(t) = \sum_{m=1}^{K} \left\{ r_m(t) \cos\left(2\pi \int_0^t \tilde{f}_m(\tau) d\tau\right) + s_m(t) \sin\left(2\pi \int_0^t \tilde{f}_m(\tau) d\tau\right)\right\} + n(t) \quad (1)$$

where $\tilde{f}_m(t)$ and $f_m(t)$ denote the estimated and true IFs for each mode. Concretely, $r_m(t)$ and $s_m(t)$ represent two demodulated modes, which are expressed as:

$$r_m(t) = A_m(t) \cos\left(2\pi \int_0^t \left(f_m(\tau) - \tilde{f}_m(\tau)\right) d\tau + \theta_m\right) \quad (2)$$

$$s_m(t) = -A_m(t) \sin\left(2\pi \int_0^t \left(f_m(\tau) - \tilde{f}_m(\tau)\right) d\tau + \theta_m\right) \quad (3)$$

It can be inferred that the demodulated signals $r_m(t)$ and $s_m(t)$ will have the narrowest bandwidth in the case of $\tilde{f}_i(t) = f_i(t)$. Then a constrained model is used to evaluate the signal bandwidth which is defined as

$$\begin{aligned} &\min_{\{r_m\},\{s_m \tilde{f}_m\}} \left\{ \sum_m \left(||r_m''(t)||_2^2 + ||s_m''(t)||_2^2 \right) \right\} \\ &\text{s.t.} x(t) = \sum_m \left(r_m(t) \cos(2\pi \int_0^t \tilde{f}_m(\tau) d\tau) \right. \\ &\qquad \left. + s_m(t) \sin(2\pi \int_0^t \tilde{f}_m(\tau) d\tau) \right) \end{aligned} \quad (4)$$

Subsequently, in order to solve the reconstruction problem, the augmented Lagrangian multiplier is used as

$$\begin{aligned} &L\left(\{r_m\}, \{s_m\}, \left\{\tilde{f}_m\right\}, \eta\right) \\ &\quad = \sum_m \left(||r_m''(t)||_2^2 + ||s_m''(t)||_2^2 \right) \\ &\qquad + \langle \eta(t), w(t) \rangle + \beta \, \|w(t)\|_2^2 \end{aligned} \quad (5)$$

$$\begin{aligned} w(t) = x(t) - \sum_m &\left(r_m(t) \cos(2\pi \int_0^t \tilde{f}_m(\tau) d\tau) \right. \\ &\left. + s_m(t) \sin(2\pi \int_0^t \tilde{f}_m(\tau) d\tau) \right) \end{aligned} \quad (6)$$

where $\eta(t)$ and β denote the Lagrangian multiplier and quadratic penalty term parameter, respectively. $\langle \bullet, \bullet \rangle$ represents the inner product function, and $w(t)$ represents the residual error term.

The solution to problem (4) is typically achieved using the alternate direction method of multipliers (ADMM) optimization algorithm [30]. Its main idea is to search the saddle point of the augmented Lagrangian $L\left(\{r_m\}, \{s_m\}, \left\{\tilde{f}_m\right\}, \eta\right)$ by alternately solving a series of sub-problems. Finally, the signal modes and IFs can be optimized with the specified initial IFs. Additional details of optimization algorithm can be found in [26].

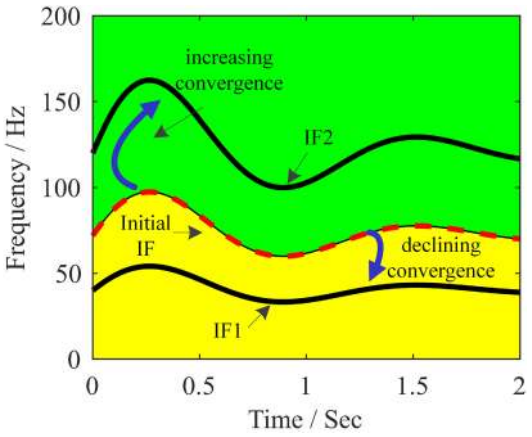

FIGURE 1. Illustration of the optimization tendency with different initial IFs.

B. CHARACTERISTIC ANALYSIS OF VNCMD

The decomposition performance of the VNCMD algorithm mainly depends on the selection of initial parameters. Apart from the decomposition number K and balance parameter β, the method of initializing IFs is also crucial for obtaining the target modes. However, few studies have been conducted to improve the performance of VNCMD in fault diagnosis. In the original VNCMD, a constant IF is only selected based on the spectral peak in different applications without distinction, which is unsuitable for the time-varying IF extraction of the target component in the entire time domain in some complicated cases. Then the fact may be that in some local time periods, constant initial IFs are good enough for optimization to the true IFs by the constraint; but in most time periods where the constant initial IFs are excessively rough compared with the true IFs, the algorithm will converge to erroneous results, and the estimated results are inevitably affected by adjacent components. Hence, a method to initialize IFs should be developed to obtain the expected modes.

Inspired by our previous study on the convergence characteristics of VMD in [31], a diagrammatic sketch is constructed to elaborate the convergence characteristics between the initialization of IFs and the decomposition results of VNCMD as shown in Fig. 1. If the initial IF locates above the IF1 in the yellow region, it will reveal a declining convergence trend associated with IF1. Contrarily, if the initial IF distribute below the IF2 in the green region, it shows an increasing convergence trend until converging to IF2. As a result, there will be a dividing line between the two modes that exhibit a different convergence trend on two sides. Based on the tendency property, the analysis signal will be adaptively decomposed in the entire frequency band provided that the initial IFs are given in a right way: (1) The initial IFs should be adjusted based on the optimal reference IF consistent with the target mode; (2) The declining trend regions can be skipped

through judgment of optimization tendency. As indicated by the arrows in the yellow region of Fig. 1, the initial IF needs to be continuously updated until it converges to IF2.

III. THE PROPOSED OTGMD METHOD FOR BEARING FAULT DIAGNOSIS UNDER VARYING SPEED CONDITIONS

A. FEATURE ISOLATION THROUGH ITERATIVE ENVELOPE ANALYSIS AND LOW-PASS FILTERING

The involved components for the diagnosis of rolling bearings are mainly related to the fault-related feature embedded in the resonance band and the fundamental SRF and its harmonics in the low-frequency band [32]. Thus, the fault-related feature can be enhanced and the interference of noise and irrelevant components can be mitigated through feature isolation for accurate bearing fault diagnosis under varying speed conditions.

In particular, a low-pass filter is initially used to extract the SRF-related information because it mainly focuses on the low-frequency band of the vibration signal. Considering that the conventional SRF and its harmonics should be observable, the range of low-frequency band is set to [0, 200 Hz] in our varying speed applications. Given that the fault characteristics are modulated into the resonance band, some demodulation methods have been explored for the extraction of fault features in recent years, among which spectral kurtosis (SK) is an effective method that discovers the presence of transient components and adaptively indicates in which frequency band the transient components occur [33]. However, it is susceptible to interference from abnormal impact and strong noise, making the location of resonance frequency inaccurate. Therefore, an iterative envelope analysis method [5], [29] is introduced for the demodulation and enhancement of fault features.

The collected vibration signal of bearing fault is composed of multiple components, including deterministic components and fault impulses. Deterministic components should be eliminated to simplify the diagnosis for enhancing the fault features. Hence, an adaptive cancellation method comprising iterative envelope and filtering is used for the demodulation and extraction of fault features. The fault enhancement for a signal $x(t)$ is described as follows:

(1) Calculate the envelope of raw signal $x(t)$ using Hilbert transform and represent it as $y^k(t)$, $k = 1, 2, \ldots$ denotes the iteration number.

(2) Subtract the direct current offset and trend term $\tilde{y}^k(t)$ from the envelope signal $y^k(t)$, which can be calculated as

$$y^k(t) = y^k(t) - \tilde{y}^k(t) \tag{7}$$

(3) Calculate the correlation of adjacent envelope signals by:

$$\gamma_k = \frac{\left|2\left\langle y^{k-1}(t)\,,\, y^k(t)\right\rangle\right|}{\left\langle y^{k-1}(t)\,,\, y^{k-1}(t)\right\rangle + \left\langle y^k(t)\,,\, y^k(t)\right\rangle} \tag{8}$$

where $\langle , \rangle$ represents the inner product operator, $y^0(t)$ represents the raw signal $x(t)$. It is easy to infer that the range of γ_k is [0, 1]. A larger correlation coefficient γ_k means that there is less difference between the adjacent envelope signals. Therefore, with the iterations of fault enhancement process, the correlation coefficient γ_k is gradually increased.

(4) Compare the correlation coefficient γ_k with a specified threshold τ, and determine the termination of iteration. When $\gamma_k > \tau$, the iteration process is terminated and the final envelope signal $y^k(t)$ is achieved, otherwise, let $x(t) = y^k(t)$ and repeat step 1 until the preset threshold τ is reached.

(5) Enhance final envelope signal $y^k(t)$ using a low-pass filter. After iterative envelope analysis, the fault features are demodulated to the low-frequency band. Another low-pass filter is applied to alleviate the noise interference and enhance the fault features. The cutoff frequency is selected based on the harmonics of FCF, which is set to [0, 500 Hz] in our applications.

In summary, the iterative envelope procedure mainly consists of two parts, namely, the removal of deterministic components from steps 1 to 4 and the enhancement of fault features in step 5. Moreover, considering the correlation coefficient is affected by the noise and interference components, the threshold τ is set to [0.9, 0.95].

B. DOMINANT IF RIDGE DETECTION

Note that the core of tacholess methods is to extract the IF ridges from the TFR of vibration signal, an effective tool named short time Fourier transform (STFT) is used for TF analysis in this paper. For a signal $X(T)$, its STFT is formed as [34]:

$$TFR(t,f) = \int_{-\infty}^{+\infty} x(\tau)\, w(t-\tau)\, e^{-2j\pi f\tau} d\tau \tag{9}$$

where $w(\,)$ represents the window function; t and f denote the time and frequency, respectively. Then, the IFs curves can be roughly observed in the TFRs. Usually, the peak search algorithm is used for the extraction of IF ridges. It is susceptible to the influence of noise and non-uniform energy distribution, thereby resulting in heavy ridge fluctuations. As a result, a handy ridge detection algorithm [26] is constructed to extract the dominant IF from the TFR in a local range, which are described as follows:

$$IF(t_n, f_n) = \arg\max_{t,f} |TFR(t,f)| \tag{10}$$

$$f_R = \arg\max_{f\in[f_R-\Delta f, f_R+\Delta f]} |TFR(t_R,f)| \tag{11}$$

$$f_L = \arg\max_{f\in[f_L-\Delta f, f_L+\Delta f]} |TFR(t_L,f)| \tag{12}$$

where Δf is the maximum frequency interval between the adjacent instants. F_R and t_R represent the frequency and instant of the rightward propagation, respectively. Equally, f_L and t_L represent the frequency and instant of the leftward propagation, respectively.

The handy ridge detection algorithm is to extract the dominant IF ridge in a local constraint range. In this way, frequency hopping at some time instants caused by the conventional peak search algorithm can be

substantially alleviated. Besides, the initial location of the highest amplitude of the TFR can also be artificially specified according to actual applications.

C. CRITERION FOR THE JUDGEMENT OF BEARING FAULT TYPE

Commonly, to ameliorate the disadvantages of traditional methods designed for constant speeds when they are used in fault detection under varying speed conditions, the order analysis is performed to eliminate the non-stationary effects of speed fluctuation by resampling method. This technique will inevitably result in interpolation errors in resampling. Hence, a non-resampling method named CFR is used to improve the diagnostic results.

For identifying the fault features in bearing detection, the FCF is usually utilized to judge different bearing components, which is defined as follows [10].

$$\mathrm{FCF}_O = \frac{N}{2}\left(1 - \frac{d}{D}\cos\varphi\right) \bullet \mathrm{SRF} = \mathrm{CFR}_O \bullet \mathrm{SRF} \quad (13)$$

$$\mathrm{FCF}_I = \frac{N}{2}\left(1 + \frac{d}{D}\cos\varphi\right) \bullet \mathrm{SRF} = \mathrm{CFR}_I \bullet \mathrm{SRF} \quad (14)$$

$$\mathrm{FCF}_B = \frac{D}{2d}\left(1 - (\frac{d}{D}\cos\varphi)^2\right) \bullet \mathrm{SRF} = \mathrm{CFR}_B \bullet \mathrm{SRF} \quad (15)$$

where N is the number of rolling elements, φ represents the contact angle, d and D denote the roller diameter and the pitch diameter of the bearing respectively. As a result, the fault frequency of outer-race FCF_O, inner-race FCF_I and rolling element FCF_B can be computed under the prior knowledge of the SRF. The CFRs of different bearing faults are characterized as the ratio of the corresponding FCF to SRF, which are constant and only determined by the geometric parameters. Hence, they can be used to identify the fault type with variable SRF, thereby avoiding the drawbacks of traditional methods.

D. THE PROPOSED OTGMD METHOD

The performance of the VNCMD algorithm introduced mostly depends on the decomposition number and the corresponding initial IFs. In particular, the VNCMD algorithm may be incapable of achieving optimized results when the initial IFs are excessively rough from the actual IFs. A handy ridge detection method is first introduced to obtain the dominant IF for the accurate input of VNCMD and alleviate the impacts caused by the incorrect estimation of initial IFs. Considering that the bearing fault signal frequently consists of several modes, a novel optimization tendency guiding strategy is constructed based on VNCMD for multicomponent extraction. The key point of OTGMD is to iteratively judge the increasing tendency of the IF in the optimization procedure to avoid setting initial IFs for the remaining target ridges.

The number of iterations cannot be determined in advance because of the interference of harmonics of SRF and FCF. A repository is constructed to store the nonstandard CFRs of different fault bearings, such as the integer multiple or fractional form of the theoretical CFR. The iteration can be terminated when the computed CFR is similar to the value in the CFRs repository. Thus, it is used as another stopping criterion in the proposed procedure. The details of the proposed OTGMD method are described as follows:

Step 1: Extract the dominant IF from the low frequency band which mainly contains SRF and its harmonics using the handy ridge detection method introduced in Section II.

Step 2: Initialize decomposition parameters: decomposition number K=1, computed CFR=1, balance parameter α is adaptively adjusted with the iterative process.

Step 3: Input the extracted IF into the VNCMD to obtain the optimal IF ω_0 (i.e. IF1) by solving the variational constraint model.

Step 4: Use the optimal IF1 ω_0 with the specified step size $\Delta\omega = l^*\omega_0$ as the initial IF $\omega^0 = \underbrace{\omega_0 + (\mathrm{CFR}-1)^*\omega_0}_{obtained\ IF} + \underbrace{l^*\omega_0}_{stepsize}$ of the next target mode. The IF is updated once times by optimizing the object function in Eq. (5). If the updated ω^1 is smaller than original ω^0, go to step 6, otherwise go to Step 5.

Step 5: Continue solving the constraint function until the stopping criterion is reached and save the optimal IF (i.e. IF2) of next target mode. Then, calculate the CFR via dividing the new IF2 by the basic IF1 and compare it with the value in the CFRs repository. The iteration is completed, and the bearing fault type can be directly determined when a similar number appears in the library. Otherwise, set the new CFR and step size $\Delta\omega = l^*\omega_0$ of obtained IF2 as the new initial IF $\omega^0 = \underbrace{\omega_0 + (\mathrm{CFR}-1)^*\omega_0}_{obtained\ IF} + \underbrace{l^*\omega_0}_{stepsize}$. When the maximum iteration number is reached, the iteration is completed, otherwise return to Step 4.

Step 6: Update the initial IF $\omega_0 + (\mathrm{CFR}-1)^*\omega_0 + l^*\omega_0$ with the increasing step size $\Delta\omega = l^*\omega_0$, and return to Step 4.

The fault diagnosis procedure by the proposed OTGMD method is illustrated in Fig. 2. Some descriptions of OTGMD strategy are described as follows.

1. In step 4, the IF optimization tendency, that is, the comparison of updated ω^1 and original ω^0 is introduced to guide the decomposition strategy. We can directly terminate the iterative optimization algorithm and update the initial IF until the declining convergence trend region is skipped when the initial IF is located in the declining trend regions, as shown in Fig. 1. The artificial setting of decomposition number in advance can be avoided through the guidance of optimization tendency. This process enables the adaptive assignment of the initial IF of concerned modes.

2. In the iterative decomposition process, some interference components with small energy may be extracted, which are named intermediate components. These components are unsuitable to be used as the initial value of

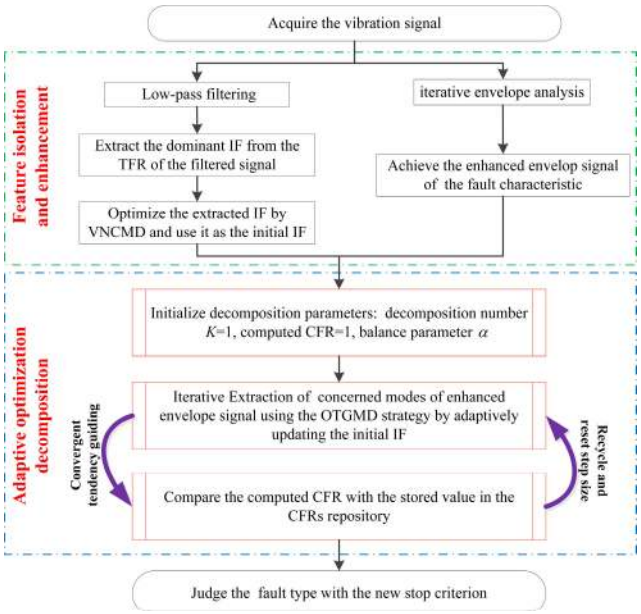

FIGURE 2. Flowchart of proposed OTGMD method for bearing fault detection with variable speed.

the next target mode because of energy dispersion and noise interference. The optimal IF1 in step 3 is constant and accurate, and we replace the initial value using the computed CFR combined with the optimal IF1, that is, $\omega^0 = \underbrace{\omega_0 + (\mathrm{CFR}-1)^*\omega_0}_{obtained\ IF} + \underbrace{l^*\omega_0}_{stepsize}$ in our procedure. This process ensures that the optimal initial IF is selected during each iteration.

3. Step size $\Delta\omega = L^*\omega_0$ of the initial IF can be adjusted to several different values at different optimization stages. In particular, step size l is appropriately reduced to ensure the decomposition effect when the computed CFR is close to the theoretical value. Otherwise, step size l can be set as relatively large to quickly search for the target components.

4. Balance parameter α is adaptively adjusted with the optimization. Given that the iterative screening process is adopted in our method, that is, only one component is extracted in each optimization process, balance parameter α can draw on the experience of the adaptive bandwidth parameter updating rule in [28] for better filtering and convergence.

IV. SIMULATIONS ANALYSIS

In order to test the performance of the proposed method for bearing fault diagnosis under varying speed conditions, a simulated model with nonlinear SRF that mimics the vibrations of a fault bearing is constructed as [35]:

$$x(t) = \sum_{k=1}^{N} U_k e^{-\beta(t-t_k)} \sin(2\pi f_r t) + \sum_{m} R_m \cos(2\pi m f_s t + \varphi_m) + n(t) \quad (16)$$

In Eq. (16), the first term of simulated model $x(t)$ denotes a series of impulses excited by a local defect of bearings, where U_k and t_k represent the time-varying amplitude and occurrence time of the kth impulse; β denotes the damping parameter, and f_r is the resonance frequency. The second term stands for the vibration components from the shafts, where f_s is the rotating frequency of the shaft. R_m and φ_m represent the amplitude and initial phase of the mth harmonic, respectively. The last term $n(t)$ represents that the signal is contaminated by strong white Gaussian noise with SNR = 0dB. Detailed parameters are displayed in Table. 1. The waveforms of noisy signal and its constituent components are sampled at a frequency of 10 kHz, as shown in Fig. 3.

TABLE 1. Parameters of simulated signal.

Parameter	f_s		f_r	β	CFR
Value	$f_s = -2*t^3 + 8*t^2 + 25$		2 kHz	1000	2.7000
Parameter	R_1	R_2	R_3	φ_1	φ_2	φ_3
Value	0.15	0.1	0.05	$\pi/6$	$-\pi/3$	$\pi/2$

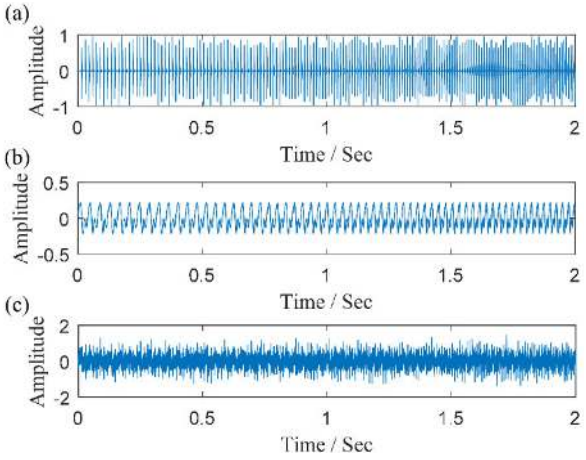

FIGURE 3. Waveforms of simulated signal: (a) repetitive impulses, (b) harmonics of shaft speed, (c) noisy signal.

It can be seen from Fig. 3(c) that the simulated signal is contaminated by strong noise, which increases the difficulty of effective features extraction. Then the feature isolation method is constructed on the noisy vibration signal. The filtered signal after low-pass filtering and the envelope signal after iterative envelope analysis can be observed in Fig. 4(a) and (c) respectively. With the low-pass filtering technique, the SRF and its harmonics are salient in the TFR of the filtered signal as shown in Fig. 4(b). Meanwhile, through iterative envelope demodulation technique, the algorithm undergoes three iterations of iterative optimization, after which the correlation coefficient γ_k is computed as 0.9552. As a result, the FCF and its harmonics can be highlighted in its TFR as described in Fig. 4(d), where the low-frequency interference components are eliminated. Then, to show the superiority of iterative envelope analysis, the conventional envelope analysis is also used in Fig. 4(e) to process the signal for enhancing the fault features. As demonstrated in Fig. 4(f), the TFR of the demodulated signal is slightly blurred and contains interference components compared with the results in Fig. 4(d).

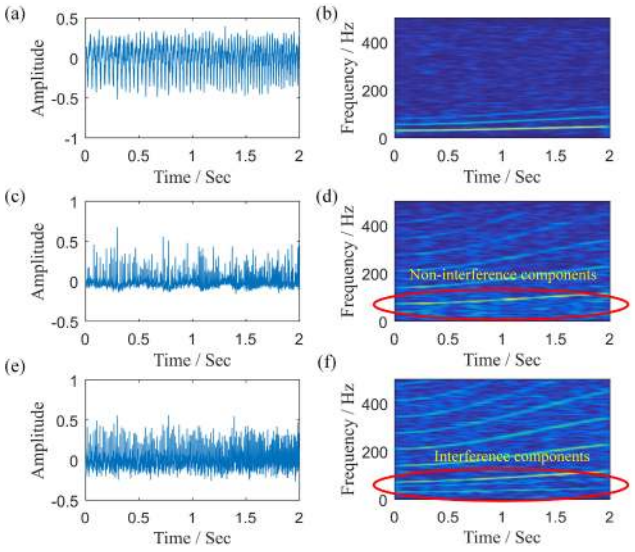

FIGURE 4. Down-sampled results of the proposed feature isolation method for simulated signal. (a) Filtered signal by low-pass filtering; (b) TFR of filtered signal; (c) Envelope signal by iterative envelope analysis; (d) TFR of iterative envelope signal; (e) Envelope signal by conventional envelope analysis; (f) TFR of single envelope signal.

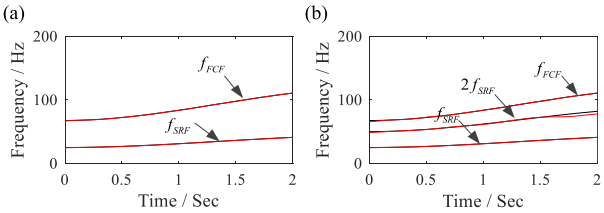

FIGURE 5. Extracted results of simulated signal. (a) Extracted IFs using the proposed OTGMD method by iterative envelope analysis; (b) Extracted IFs using the proposed OTGMD method by conventional envelope analysis (black: true; red: estimated).

Actually, to improve the computational efficiency, the down-sampling technique is applied here with the frequency of 1000Hz. Therefore, Fig. 4 reveals the down-sampled results of proposed feature isolation method for simulated signal.

Next, the OTGMD method is utilized for dominant IF extraction. Here, the first extracted IF in the low-frequency band of Fig. 4(b) is SRF, and then is optimized by VNCMD as the initial input of next mode of envelope signal in Fig. 4(d). To accelerate the optimization process of the OTGMD algorithm, the step size $\Delta\omega = l^*\omega_0$ undergoes three stages: factors l is set to 0.4 when the computed CFR is less than 0.5, set to 0.2 when the computed CFR is less than 0.8, and lastly set to 0.15 until the stop condition is reached after each update. Eventually, the extraction results are shown in Fig. 5. It can be seen from Fig. 5(a) that the algorithm undergoes one iteration of optimization, after which the estimated FCF is approximately coincident with the true one. The ultimate CFR is computed as 2.7050 with average relative error of 0.18% compared with the theoretical value of 2.7000. Subsequently, the same OTGMD method is applied in Fig. 4(e) and (f). The results are displayed in Fig. 5(b), where two components are adaptively extracted as 2SRF and FCF respectively.

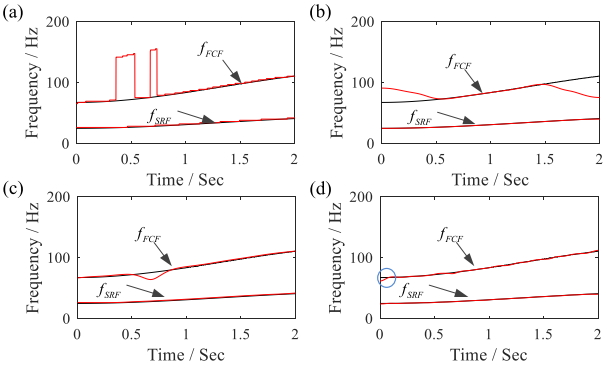

FIGURE 6. Extracted results of other methods for simulated signal. (a) Extracted IFs using the conventional peak search algorithm; (b) Extracted IFs using the original VNCMD method with constant IFs; (c) Extracted IFs using the ridge detection method; (d) Extracted IFs using the improved VNCMD method with varying IFs (black: true; red: estimated).

Besides, the extracted component of 2SRF displays noticeable jumps and the boundaries are broken because of noise. The ultimate CFR is calculated as 2.6820, which shows slightly larger errors.

Therefore, we can certainly enhance the IF features (SRF and FCF) and mitigate the interference of noise and irrelevant components through feature isolation using iterative envelope analysis. On another note, the proposed OTGMD method can constantly converge to an appropriate result regardless of the influence of interference components. Thus, the proposed OTGMD method combined with iterative envelope demodulation technology shows its potential in fault diagnosis. The use of CFR as a new stopping criterion effectively avoids the choice of initial decomposition number and adaptively selects the meaningful components.

Further, to demonstrate the advantages of optimization tendency guiding decomposition strategy in OTGMD, the conventional peak search algorithm, the original VNCMD method and improved VNCMD method are performed as shown in Fig. 6. The result of peak search algorithm in Fig. 6(a) presents severe hopping in the FCF ridge due to that it only focuses on the highest energy point and ignores smoothness. Therefore, it cannot reflect the actual IF curve and is invalid for bearing fault diagnosis in our experiment. Then, the extracted IFs using the original VNCMD method are displayed in Fig. 6(b). The constant initial IFs are set to 32 Hz and 86 Hz according to the average values of the TF ridges, respectively. The results reveals that the boundary of the extracted FCF displays large jumps because the constant initial IF is far from the true value at the boundary. Finally, the improved VNCMD method using ridge detection is applied to mitigate the effect of initial IF. As demonstrated in Fig. 6(c), although the FCF estimated by the tractable ridge detection method exhibits some errors, it is remarkably improved compared with the results of the peak search algorithm and is optimized by the VNCMD method, as shown in Fig. 6(d). The FCF shows some deviations at the boundary, as indicated by the blue circle. The CFR with the SRF

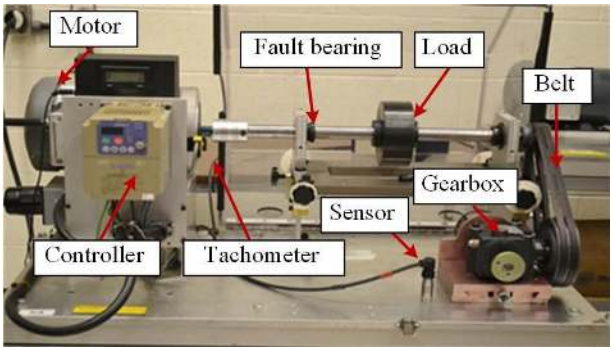

FIGURE 7. Experimental set-up.

and FCF is calculated as 2.6871, which is slightly worse compared with the proposed method. Although the improved VNCMD method uses a recursive framework to gradually extract signal modes, it still needs to feed the corresponding IFs of all modes using ridge detection. Hence, it has high requirements for the accuracy of all extracted ridges. The proposed method only needs to extract the dominant IF and adaptively set the initial IFs of meaningful modes. Therefore, the proposed method is suitable for signal extraction under strong background noise.

In summary, the feature isolation method can generate a clear and concentrated TFR for the extraction of SRF-related and FCF-related ridges. The comparison results demonstrate the effectiveness of OTGMD in accurately extracting FCF features without setting the initial IFs in advance. The proposed method successfully diagnoses the fault type under varying speed conditions and is superior to the existing methods.

V. EXPERIMENTAL VALIDATION

In this section, the performance of the proposed method is further validated in practical applications, the OTGMD method combined with feature isolation is used to analyze the experimental bearing vibration data under varying speed conditions. The overview of experimental setup for data acquisition is shown in Fig. 7. Two bearings of type RE16K are mounted to support the shaft which is driven by a motor. The rotational speed can be controlled by an AC inverter and the fault bearing is installed at the left side. An accelerometer is used to collect the vibration signal and the rotational speed can be roughly measured by a tachometer. Two experiments for vibration data analysis with bearing inner and outer defects are carried out, respectively.

A. BEARING OUTER RACE FAULT IDENTIFICATION

In this subsection, the vibration signal of bearing outer race fault is collected from the rotating machine. During the operation of rotating machine, the vibration data are sampled at a frequency of 20 kHz and the shaft rotational speed is gradually increased. Other detailed structural parameters of the test bearing are listed in Table. 2. The time waveform of the raw vibration signal is shown in Fig. 8. Generally, we barely see any useful information from the original signal, thus hindering effective fault diagnosis.

TABLE 2. Parameters of outer race fault bearing.

Parameter	Pitch diameter(mm)	Ball diameter(mm)	Ball numbers	CFR
Value	38.52	7.94	9	3.5000

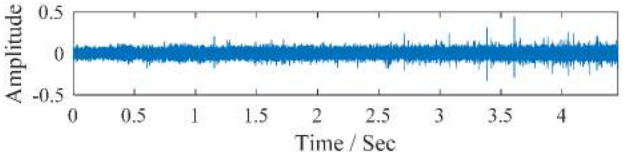

FIGURE 8. Waveforms of outer race defect vibration signal.

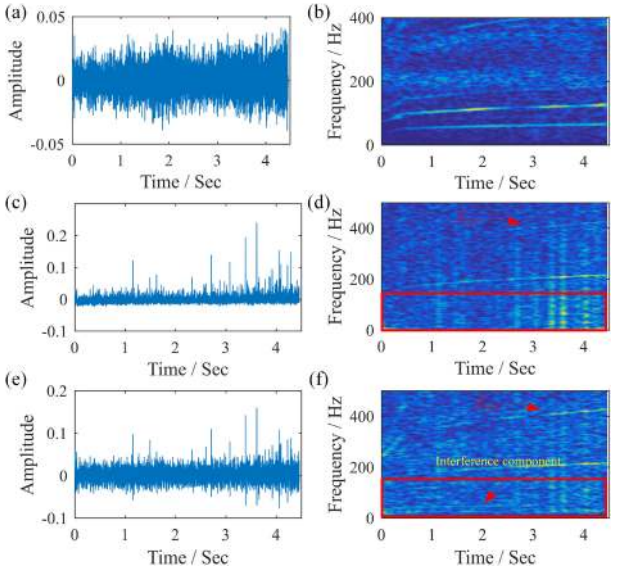

FIGURE 9. Down-sampled results of the proposed feature isolation method for outer race fault signal. (a) Filtered signal by low-pass filtering; (b) TFR of filtered signal; (c) Envelope signal by iterative envelope analysis; (d) TFR of iterative envelope signal; (e) Envelope signal by conventional envelope analysis; (f) TFR of single envelope signal.

Similarly, the noisy vibration signal is first processed through feature isolation to reveal the interested components. The down-sampled results of filtered, iterative envelope, and conventional envelope signals are illustrated in Fig. 9. In the iterative analysis, the algorithm undergoes two iterations, and correlation coefficient γ_k is calculated as 0.9325. Although the fault characteristics are enhanced compared with the conventional envelope analysis in Fig. 9(d) and (f), the iterative envelope analysis eliminates the low-frequency interference component and its harmonics because of one more iterative process, as marked by the solid rectangle. Besides, due to the interference of strong background noise, it is difficult to identify the FCF directly.

First, the OTGMD method is performed on enhanced signals in Fig. 9. As shown in the result of Fig. 10(a), we can observe that the proposed method clearly tracks the dominant IF exactly as the optimized SRF. The SRF is fed into the iterative envelope signal to adaptively search the FCF under

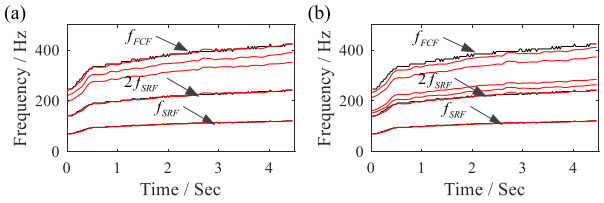

FIGURE 10. Extracted results of outer race fault signal. (a) Extracted IFs using the proposed OTGMD method by iterative envelope analysis; (b) Extracted IFs using the proposed OTGMD method by conventional envelope analysis (black: true; red: estimated).

the guidance of convergence tendency. Similarly, the step size is adjusted in three stages to accelerate the search process. Factor l is set to 0.25, 0.2, and 0.15 when the computed CFR is less than 0.5, 0.8 and meets the stop condition, respectively. The extracted FCF is generally consistent with the actual one. Although it extracts some false and irrelevant components during optimization, it continuously searches until the stop condition is met and the right component is located. The computed CFR is 3.5107 after iterative searching. This finding indicates that the computed CFR of 3.5005 is approximately close to the theoretical value of 3.5000 with average relative error is 0.31%. Therefore, the powerful performance of the proposed OTGMD method is demonstrated in outer race fault diagnosis.

The OTGMD method is combined with conventional envelope signal in Fig. 9(e) and (f). As shown in the result of Fig. 10(b), the CFR is calculated as 3.3832, and the average relative error is 3.33% compared with the theoretical value of 3.5000. The result evidently deviates from the standard values and is disturbed by many irrelevant components, thereby reducing the accuracy of diagnosis. This condition confirms that feature isolation can effectively enhance the characteristics of signals.

For comparison, the methods used in simulation analysis are applied to extract and optimize the IFs. The results of conventional peak search algorithm are shown in Fig. 11(a), where the ridges show huge frequency jump patterns for the signal components because of blurry TFR. Then, the original VNCMD in which its constant initial IFs are specified as 107 and 375 Hz is applied to extract the SRF and FCF. As shown in Fig. 11(b), the accuracy of SRF is improved, but the boundary effect still exists. A serious error occurs at the FCF because the actual IF has a large fluctuation range. Hence, the computed CFR is incorrect and incapable of effective fault diagnosis of outer race bearings under varying speed conditions.

The extraction results of the improved VNCMD method are exhibited in Fig. 11(c) and (d). In the low-frequency band, the energy of SRF is dominant and can be accurately extracted. However, the initial IF fails to be accurately extracted because the fault feature component is submerged by strong noise, thereby resulting in large errors of the subsequent input. Hence, unexpected components are extracted that hinder the judgment of fault type. The proposed method needs to extract the dominant SRF component and adaptively

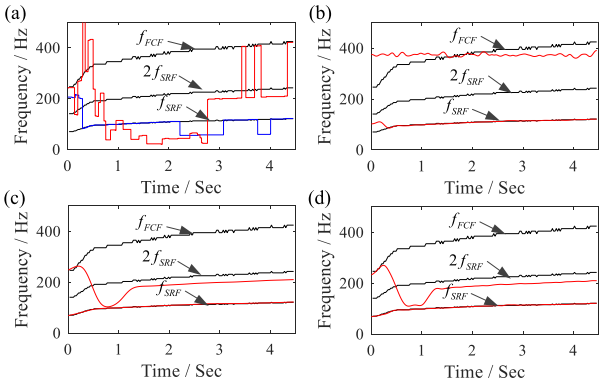

FIGURE 11. Extracted results of other methods for outer race fault signal. (a) Extracted IFs using the conventional peak search algorithm; (b) Extracted IFs using the original VNCMD method with constant IFs; (c) Extracted IFs using the ridge detection method; (d) Extracted IFs using the improved VNCMD method with varying IFs (black: true; red and blue: estimated).

TABLE 3. Parameters of inner race fault bearing.

Parameter	Pitch diameter(mm)	Ball diameter(mm)	Ball numbers	CFR
Value	38.52	7.94	9	5.4300

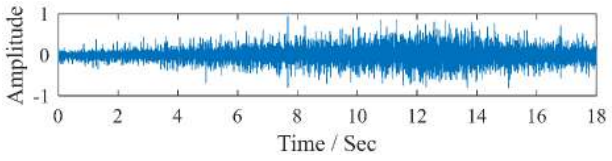

FIGURE 12. Waveforms of inner race defect vibration signal.

set the input of subsequent components to avoid the problem.

The proposed feature isolation method can depict clear TFR for the characteristic components, and the OTGMD method can adaptively optimize each component. The analysis results successfully validate that the proposed method is superior to other methods.

B. BEARING INNER RACE FAULT IDENTIFICATION

In this subsection, the proposed method is further verified using a bearing with the inner race fault under the process of acceleration and deceleration. The experiment is carried out in the device in Fig. 7 by replacing the left bearing with inner race fault. Table. 3 displays other parameters of inner race fault bearing and the vibration data are sampled at 12 kHz. As shown in Fig. 12, the amplitude of the collected vibration signal increases and decreases with the change of the SRF.

The feature isolation method is performed on the raw signal to enhance the concerned features. Similar to the above tests, the down-sampled signals and their TFRs are illustrated in Fig. 13. The resolution of each TFR is sufficient to clearly reveal the signal characteristics, especially at the low-frequency band. The results of iterative envelope analysis in Fig. 13(d) show fewer low-frequency

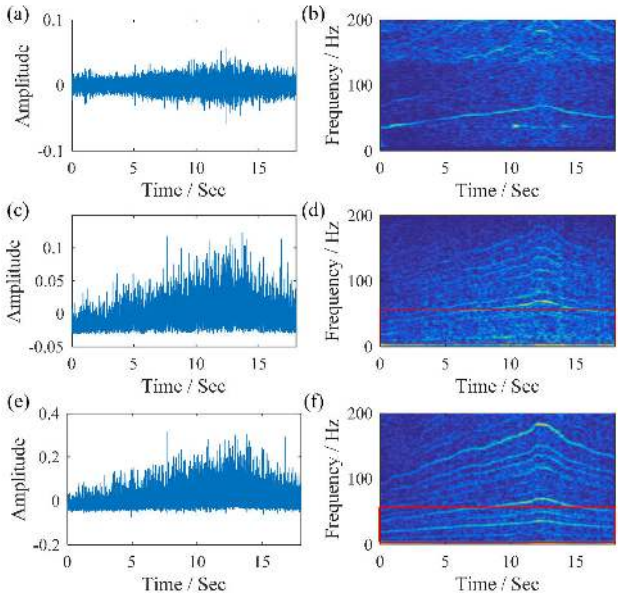

FIGURE 13. Down-sampled results of the proposed feature isolation method for inner race fault signal. (a) Filtered signal by low-pass filtering; (b) TFR of filtered signal; (c) Envelope signal by iterative envelope analysis; (d) TFR of iterative envelope signal; (e) Envelope signal by conventional envelope analysis; (f) TFR of single envelope signal.

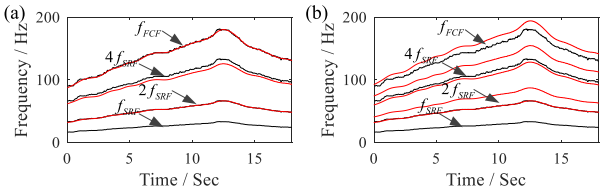

FIGURE 14. Extracted results of inner race fault signal. (a) Extracted IFs using the proposed OTGMD method by iterative envelope analysis; (b) Extracted IFs using the proposed OTGMD method by conventional envelope analysis (black: true; red: estimated).

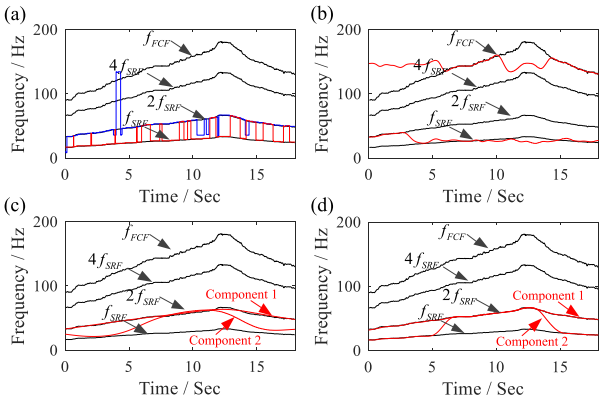

FIGURE 15. Extracted results of other methods for inner race fault signal. (a) Extracted IFs using the conventional peak search algorithm; (b) Extracted IFs using the original VNCMD method with constant IFs; (c) Extracted IFs using the ridge detection method; (d) Extracted IFs using the improved VNCMD method with varying IFs (black: true; red and blue: estimated).

interference components compared with the results of conventional envelope analysis in Fig. 13(f). Hence, the fault features are sufficiently enhanced for reliable identification of IF ridge information from the TFR using the proposed feature isolation method.

The extracted results are exhibited in Fig. 14(a) after two iterations of the OTGMD method, and correlation coefficient γ_k is computed as 0.9748. The dominant IF for input is 2SRF, and the last extracted component is the FCF. Hence, the final calculated CFR is 2.7246 with average relative error of 0.35%, which is approximately half of the theoretical one in Table 3. In convergence trend optimization, step size factor l is set to 0.3, 0.2, and 0.15 in three stages, respectively, similar to the previous tests. This finding validates the effectiveness of CFRs repository in avoiding the interference of harmonics of SRF and FCF. The iteration is terminated after two optimization extractions when the computed CFR is half of the theoretical value. As shown in Fig. 14(b), the OTGMD method combined with conventional envelope analysis tracks some interference components, thereby increasing the consumption of the algorithm and results in misjudgment. The final CFR is computed as 2.9202, which is far from half of the theoretical one in Table 3.

Furthermore, comparisons of the extracted IFs by some common methods are shown in Fig. 15. As represented in Fig. 15(a) and (b), due to the uneven distribution of energy, the first two dominant components by the peak search method show large fluctuations between SRF and its harmonic. When it comes to the original VNCMD method with the constant initial IFs of 27 Hz and 144 Hz, the results of the first two dominant components displays serious errors under the interference of irrelevant components. The terrible results lead to the wrong CFR and fail to perform the accurate judgement of fault type.

Finally, Fig. 15(c) and (d) reveal the extraction results of improved VNCMD method. In low frequency band, the energy of SRF is dominant and it can be extracted accurately as noted by redline (component 1) in Fig. 15(c) and (d). The initial IF cannot be accurately extracted because the fault feature component is submerged by several interference components and the first two dominant components do not contain FCF, thereby leading to large errors in subsequent optimization. Thus, some unexpected components may be extracted, and the decomposition process needs artificial analysis and judgment, which increase the difficulty of fault diagnosis. Therefore, these test results verify the effectiveness and superiority of the proposed method for detecting bearing faults under varying speed conditions.

VI. CONCLUSION

In this study, a feature isolation method and a novel decomposing strategy (i.e., OTGMD) are developed to enhance the characteristics of concerned IFs and accurately feed initial IFs of extracted components for the fault diagnosis of bearings under varying speed conditions. First, the dominant IF is estimated in the low-frequency band through ridge detection method and then refined via the raw VNCMD method. Subsequently, in order to reduce the influence of noise and facilitate the extraction of subsequent components, the fault

characteristic is augmented with iterative envelope analysis. Then, OTGMD initializes the IF of each component through an iterative TFR-independent procedure. Finally, the iterative extraction process will automatically terminate when the stopping criterion are satisfied. It avoids the extraction of the redundant feature components and is free of human participation. The proposed method can create a high-resolution TFR for each concerned component and adaptively set the initial IFs of the meaningful modes in the entire frequency band. It effectively overcomes the poor TF resolution of traditional envelope method and the difficulty of raw VNCMD parameter selection.

Simulated and experimental tests clearly validate that OTGMD can accurately extract SRF and FCF, thereby providing a promising solution for bearing fault diagnosis under varying speed conditions. The comparisons also verify the effectiveness and superiority of the proposed method for target ridge extraction and fault discrimination.

ACKNOWLEDGMENT

The authors would like to thank the Lab E026 in University of Ottawa for data collection.

REFERENCES

[1] J. Li, M. Li, and J. Zhang, "Rolling bearing fault diagnosis based on time-delayed feedback monostable stochastic resonance and adaptive minimum entropy deconvolution," *J. Sound Vibrat.*, vol. 401, pp. 139–151, Aug. 2017.

[2] W. Teng, X. Ding, Y. Zhang, Y. Liu, Z. Ma, and A. Kusiak, "Application of cyclic coherence function to bearing fault detection in a wind turbine generator under electromagnetic vibration," *Mech. Syst. Signal Process.*, vol. 87, pp. 279–293, Mar. 2017.

[3] Z. Wang, L. Zheng, J. Wang, and W. Du, "Research on novel bearing fault diagnosis method based on improved krill herd algorithm and kernel extreme learning machine," *Complexity*, vol. 2019, pp. 1–19, Nov. 2019, doi: 10.1155/2019/4031795.

[4] Z. Wang, W. Du, J. Wang, J. Zhou, X. Han, Z. Zhang, and L. Huang, "Research and application of improved adaptive MOMEDA fault diagnosis method," *Measurement*, vol. 140, pp. 63–75, Jul. 2019.

[5] A. Ming, W. Zhang, Z. Qin, and F. Chu, "Fault feature extraction and enhancement of rolling element bearing in varying speed condition," *Mech. Syst. Signal Process.*, vols. 76–77, pp. 367–379, Aug. 2016.

[6] S. Wang, X. Chen, C. Tong, and Z. Zhao, "Matching synchrosqueezing wavelet transform and application to aeroengine vibration monitoring," *IEEE Trans. Instrum. Meas.*, vol. 66, no. 2, pp. 360–372, Feb. 2017.

[7] Y. Lei, J. Lin, M. J. Zuo, and Z. He, "Condition monitoring and fault diagnosis of planetary gearboxes: A review," *Measurement*, vol. 48, pp. 292–305, Feb. 2014.

[8] H. Cao, F. Fan, K. Zhou, and Z. He, "Wheel-bearing fault diagnosis of trains using empirical wavelet transform," *Measurement*, vol. 82, pp. 439–449, Mar. 2016.

[9] Y. Liu, B. He, F. Liu, S. Lu, and Y. Zhao, "Feature fusion using kernel joint approximate diagonalization of eigen-matrices for rolling bearing fault identification," *J. Sound Vibrat.*, vol. 385, pp. 389–401, Dec. 2016.

[10] R. B. Randall and J. Antoni, "Rolling element bearing diagnostics—A tutorial," *Mech. Syst. Signal Process.*, vol. 25, no. 2, pp. 485–520, 2011.

[11] R. B. Randall,"A history of cepstrum analysis and its application to mechanical problems," *Mech. Syst. Signal Process.*, vol. 97, pp. 3–19, Dec. 2017.

[12] S. Zhang, Z. Sun, M. Wang, J. Long, Y. Bai, and C. Li, "Deep fuzzy echo state networks for machinery fault diagnosis," *IEEE Trans. Fuzzy Syst.*, to be published.

[13] Y. Lei, J. Lin, Z. He, and M. J. Zuo, "A review on empirical mode decomposition in fault diagnosis of rotating machinery," *Mech. Syst. Signal Process.*, vol. 35, nos. 1–2, pp. 108–126, Feb. 2013.

[14] Z. Wang, J. Wang, W. Cai, J. Zhou, W. Du, J. Wang, G. He, and H. He, "Application of an improved ensemble local mean decomposition method for gearbox composite fault diagnosis," *Complexity*, vol. 2019, pp. 1–17, May 2019.

[15] P. Borghesani, P. Pennacchi, S. Chatterton, and R. Ricci, "The velocity synchronous discrete Fourier transform for order tracking in the field of rotating machinery," *Mech. Syst. Signal Process.*, vol. 44, nos. 1–2, pp. 118–133, Feb. 2014.

[16] T. Wang, M. Liang, J. Li, and W. Cheng, "Rolling element bearing fault diagnosis via fault characteristic order (FCO) analysis," *Mech. Syst. Signal Process.*, vol. 45, no. 1, pp. 139–153, Mar. 2014.

[17] Y. Wang, G. Xu, A. Luo, L. Liang, and K. Jiang, "An online tacholess order tracking technique based on generalized demodulation for rolling bearing fault detection," *J. Sound Vibrat.*, vol. 367, pp. 233–249, Apr. 2016.

[18] T. Wang, M. Liang, J. Li, W. Cheng, and C. Li, "Bearing fault diagnosis under unknown variable speed via gear noise cancellation and rotational order sideband identification," *Mech. Syst. Signal Process.*, vols. 62–63, pp. 30–53, Oct. 2015.

[19] Y. Wang, G. Xu, Q. Zhang, D. Liu, and K. Jiang, "Rotating speed isolation and its application to rolling element bearing fault diagnosis under large speed variation conditions," *J. Sound Vibrat.*, vol. 348, pp. 381–396, Jul. 2015.

[20] M. Zhao, J. Lin, X. Xu, and Y. Lei, "Tacholess envelope order analysis and its application to fault detection of rolling element bearings with varying speeds," *Sensors*, vol. 13, no. 8, pp. 10856–10875, Aug. 2013.

[21] H. Huang, N. Baddour, and M. Liang, "Bearing fault diagnosis under unknown time-varying rotational speed conditions via multiple time-frequency curve extraction," *J. Sound Vibrat.*, vol. 414, pp. 43–60, Feb. 2018.

[22] X. Jiang and S. Li, "A dual path optimization ridge estimation method for condition monitoring of planetary gearbox under varying-speed operation," *Measurement*, vol. 94, pp. 630–644, Dec. 2016.

[23] X. Jiang, S. Li, and Q. Wang, "A study on defect identification of planetary gearbox under large speed oscillation," *Math. Problems Eng.*, vol. 2016, pp. 1–18, 2016.

[24] S. Chen, Z. Peng, Y. Yang, X. Dong, and W. Zhang, "Intrinsic chirp component decomposition by using Fourier Series representation," *Signal Process.*, vol. 137, pp. 319–327, Aug. 2017.

[25] S. Chen, X. Dong, G. Xing, Z. Peng, W. Zhang, and G. Meng, "Separation of overlapped non-stationary signals by ridge path regrouping and intrinsic chirp component decomposition," *IEEE Sensors J.*, vol. 17, no. 18, pp. 5994–6005, Sep. 2017.

[26] S. Chen, X. Dong, Z. Peng, W. Zhang, and G. Meng, "Nonlinear chirp mode decomposition: A variational method," *IEEE Trans. Signal Process.*, vol. 65, no. 22, pp. 6024–6037, Nov. 2017.

[27] W. Guo, X. Jiang, N. Li, J. Shi, and Z. Zhu, "A coarse TF ridge-guided multi-band feature extraction method for bearing fault diagnosis under varying speed conditions," *IEEE Access*, vol. 7, pp. 18293–18310, 2019.

[28] S. Chen, Y. Yang, Z. Peng, X. Dong, W. Zhang, and G. Meng, "Adaptive chirp mode pursuit: Algorithm and applications," *Mech. Syst. Signal Process.*, vol. 116, pp. 566–584, Feb. 2019.

[29] A. Ming, W. Zhang, Z. Qin, and F. Chu, "Envelope calculation of the multi-component signal and its application to the deterministic component cancellation in bearing fault diagnosis," *Mech. Syst. Signal Process.*, vols. 50–51, pp. 70–100, Jan. 2015.

[30] W. Shi, Q. Ling, K. Yuan, G. Wu, and W. Yin, "On the linear convergence of the ADMM in decentralized consensus optimization," *IEEE Trans. Signal Process.*, vol. 62, no. 7, pp. 1750–1761, Apr. 2014.

[31] X. Jiang, C. Shen, J. Shi, and Z. Zhu, "Initial center frequency-guided VMD for fault diagnosis of rotating machines," *J. Sound Vibrat.*, vol. 435, pp. 36–55, Nov. 2018.

[32] J. Obuchowski, A. Wylomanska, and R. Zimroz, "Selection of informative frequency band in local damage detection in rotating machinery," *Mech. Syst. Signal Process.*, vol. 48, nos. 1–2, pp. 138–152, Oct. 2014.

[33] J. Antoni and R. Randall, "The spectral kurtosis: Application to the vibratory surveillance and diagnostics of rotating machines," *Mech. Syst. Signal Process.*, vol. 20, no. 2, pp. 308–331, Feb. 2006.

[34] H. Gao, L. Liang, X. Chen, and G. Xu, "Feature extraction and recognition for rolling element bearing fault utilizing short-time Fourier transform and non-negative matrix factorization," *Chin. J. Mech. Eng.*, vol. 28, no. 1, pp. 96–105, Jan. 2015.

[35] J. Shi, M. Liang, and Y. Guan, "Bearing fault diagnosis under variable rotational speed via the joint application of windowed fractal dimension transform and generalized demodulation: A method free from prefiltering and resampling," *Mech. Syst. Signal Process.*, vols. 68–69, pp. 15–33, Feb. 2016.

XINGXING JIANG received the B.S. and Ph.D. degrees in vehicle engineering from the Nanjing University of Aeronautics and Astronautics, Nanjing, China, in 2008 and 2016, respectively. He is currently an Associate Professor with the School of Rail Transportation, Soochow University, China. His current research interests include machinery condition monitoring and fault diagnosis, and time–frequency analysis.

WENJUN GUO received the B.S. degree in electrical engineering and automation from Soochow University, Suzhou, China, in 2017, where he is currently pursuing the M.S. degree in testing and measuring technology and instrumentation. His current research interests include signal processing and machinery fault diagnosis.

GUIFU DU was born in Shandong, China. He received the B.E. and Ph.D. degrees from the China University of Mining and Technology, Xuzhou, China, in 2012 and 2017, respectively. He joined the School of Rail Transportation, Soochow University, Suzhou, China, in September 2017, as a Lecturer. His current research interests include fault diagnosis of DC traction power systems and railway electrification.

JUANJUAN SHI received the B.S. and M.S. degrees in mechanical engineering from Northwest A&F University, Shaanxi, China, in 2008 and 2011, respectively, and the Ph.D. degree in mechanical engineering from the University of Ottawa, Ontario, Canada, in 2015. From 2012 to 2015, she was a Teaching Assistant with the University of Ottawa. Since 2016, she has been an Associate Professor with the School of Urban Rail Transportation, Soochow University, China. Her research interests include rotating machinery condition monitoring, vibration control, and digital signal processing.

ZHONGKUI ZHU received the B.S. degree in automobile and tractor (Automobile) and the M.S. degree in vehicle engineering from Hefei Polytechnic University, in 1997 and 2002, respectively, and the Ph.D. degree in instrument science and technology from the University of Science and Technology of China, in 2005. He is currently a Professor with the School of Rail Transportation, Soochow University. His research interests include vehicle system dynamics and control, vibration measurement, and signal processing.